[5] R. E. Collin, Foundations for Microwave Engineering. New York: McGraw Hill, 1966, pp. 329–336.

[6] R. Aston, "Techniques for increasing the bandwidth of a TM_{010}-mode power combiner," *IEEE Trans. Microwave Theory Tech.*, vol. MTT-27, pp. 479–482, May 1979.

[7] K. Kurokawa, "The single-cavity multiple-device oscillator," *IEEE Trans. Microwave Theory Tech.*, vol. MTT-19, pp. 793–801, Oct. 1971.

[8] K. Kurokawa, "An analysis of Rucker's multidevice symmetrical oscillator," *IEEE Trans. Microwave Theory, Tech.*, vol. MTT-18, pp. 967–968, Nov. 1970.

[9] M. Maeda, K. Kimura, and H. Kodera, "Design and performance of *X*-band oscillators with GaAs Schottky-gate field-effect transistors," *IEEE Trans. Microwave Theory Tech.*, vol. MTT-23, pp. 661–667, Aug. 1975.

[10] K. J. Russel, "Microwave power combining techniques," *IEEE Trans. Microwave Theory Tech.*, vol. MTT-27, pp. 472–478, May 1979.

Andrzej Materka was born in Łęczyca, Poland, on November 18, 1949. He received the M.Sc. degree in radio engineering from Warsaw Technical University and the Ph.D. degree in technical sciences from Łódź Technical University, in 1972 and 1979, respectively.

From 1972 to 1974 he worked for the Radio and Television Broadcasting Stations, Łódź, on transmitters and circuits for space division of video signals. Later, he joined the Institute of Electronics, Łódź Technical University, to serve as a Research and Teaching Assistant on testability of analog circuits, CAD design, and semiconductor devices modeling. Since 1979 he has been a Lecturer at the same university.

In 1980 he was granted a Japanese Government scholarship and joined the Research Institute of Electronics, Shizuoka University, Hamamatsu, Japan. His current research interests include power-combining techniques and FET oscillators.

Shizuo Mizushina (S'60–M'66) was born in Hamamatsu, Japan, on August 10, 1933. He received the B.Eng. degree from Shizuoka University, Hamamatsu, in 1957, and the M.Sc. and Ph.D. degrees from Ohio State University, Columbus, in 1962 and 1964, respectively.

From 1957 to 1960 he was a Research Assistant and Lecturer at Shizuoka University. From 1964 to 1965 he was a Member of the Technical Staff at the Bell Telephone Laboratories, Murray Hill, NJ. In 1965 he returned to Shizuoka University where he is a Professor at the Research Institute of Electronics. He has worked on millimeter-wave magnetrons, gigabit-pulse regenerators, solid-state oscillators, and device-circuit interaction problems. His current research interests are concerned with microwave power-combining techniques, microwave thermography, and medical electronics.

Dr. Mizushina is a member of the Institution of Electronics and Communication Engineers of Japan, the Japan Society of Medical Electronics and Biological Engineering, and Sigma Xi.

Monolithic Integration of a Dielectric Millimeter-Wave Antenna and Mixer Diode: An Embryonic Millimeter-Wave IC

CHINGCHI YAO, STEVEN E. SCHWARZ, SENIOR MEMBER, IEEE, AND B. J. BLUMENSTOCK

***Abstract* —A monolithic silicon integrated circuit consisting of a mixer diode and an all-dielectric receiving antenna has been built and tested at 85 GHz. Radiation is coupled into the device optically with a coupling loss of 2.7 dB. No external metal structure is required for coupling. The design can be used efficiently at considerably higher frequencies, and can be elaborated into more complex integrated circuits. From measurements of video responsivity the losses of various parts of the device are estimated. A simple theory of conversion efficiency is found to agree well with experiments; this theory is then used to predict the performance of improved versions of the device. The conversion efficiency obtained with this demonstration device is low; it is shown, however, that acceptable conversion efficiencies can be obtained with a more advanced diode fabrication technology using epitaxial Si or GaAs. Integrated millimeter-wave receivers of this kind should be suitable for short-path terrestrial communications, in applications where compactness and low cost are required.**

Manuscript received December 30, 1981; revised March 2, 1982. This work was sponsored in part by the U.S. Army Research Office under Grant DAAG29-79-C-0134, in part by the National Science Foundation under Grant ECS-8009033, in part by the Air Force Office of Scientific Research, United States Air Force under Contract F49620-79-C-0178, and in part by the U.S. Army Mobility Equipment Research and Development Command under Contract DAAK70-80-C-0134.

The authors are with the Department of Electrical Engineering and Computer Sciences, and the Electronics Research Laboratory, University of California, Berkeley, CA 94720.

I. Introduction

A NUMBER OF different waveguide technologies are available for use in the "near-millimeter" regime of 100–300 GHz. These include conventional hollow metal waveguide, fin line, various strip lines, microstrip, dielectric image guide, and all-dielectric guides. All of these guides are subject, to a greater or lesser degree, to the typical problems of this frequency range, such as the small dimensions of single-mode guiding structures and the lossiness of metals due to skin effect and surface roughness. As compared with other guides, all-dielectric guides have several advantages. They are free of metallic losses, except perhaps for losses in small metal coupling structures. When the dielectric is a semiconductor, guides of suitable dimensions can be fabricated easily by photolithography. Moreover, semiconductor devices can be constructed in the guide material to create monolithic integrated structures. An interesting feature of this technology is that its advantages tend to increase with increasing frequency. As frequency increases, fabrication of the structures becomes more convenient, and unit cost decreases because more devices can be obtained from each wafer. Dielectric losses also become less of a problem as frequency increases. Assuming that these arise from the conductivity of the semiconductor, an upper limit of the power loss coefficient is given by $\alpha \doteq \sigma\sqrt{\mu/\epsilon}$ where σ, μ, and ϵ are the conductivity, magnetic permeability, and electric permittivity, respectively. Thus α is nearly independent of frequency and the loss per guide wavelength decreases as $1/f$. (For 1000 ohm·cm silicon $\alpha \doteq 0.5$ dB/cm, which amounts to about 0.02 dB per guide wavelength at 300 GHz.)

It seems possible to use these dielectric guides as a basis for other devices such as hybrid couplers, filters, and resonators. This approach leads toward a near-millimeter-wave IC technology: for example, it should not be too difficult to assemble a hybrid coupler and balanced mixer in monolithic form, and perhaps IF amplifiers as well. It seems probable that the performance of such IC's will be somewhat less than the present state-of-the-art because of fabrication constraints. In return, however, one expects to gain advantages in terms of ruggedness, compactness, and low cost, as has been pointed out in earlier work [1]. In the present paper we report an early step toward this type of integrated circuit, a monolithic assembly consisting of a dielectric antenna, waveguide, and a Schottky mixer diode. This is, we believe, the first monolithic integration of a mixer diode with a self-contained, efficient antenna. The actual performance of our device is rather poor, but this is a consequence of the primitive diode technology that was used. Our purpose in this paper is not to demonstrate a finished practical device, but rather to indicate a novel way in which practical devices can be achieved.

II. Device Description

A diagram of the device is shown in Fig. 1(a). The antenna component is similar to a design described earlier [2]. It consists of a tapered dielectric rod etched from a silicon wafer. A V-shaped metallic coupler serves to feed the guided radiation into the diode located at its apex. The received polarization is that with electric field in the plane of the V. In the earlier design the silicon membrane supported the low-frequency leads. The present design places the two low-frequency leads (which are in the form of coplanar strips) closer together so that they are over the dielectric rod rather than on the supporting membrane (Fig. 1(b)). This modification works as well as the previous design, according to scale-model experiments at 4.3 GHz. This suggests that electromagnetic fields are concentrated within the acute angle of the V-coupler; moving the leads, which are outside the coupler closer to the vertex, thus does not significantly affect the field distribution. In microwave simulation the antenna shows a single-lobed pattern along the axis of the V, and this is also the case for the actual device tested at 85 GHz. The observed pattern at 85 GHz has beam angles full width at half maximum (FWHM) of 49° in the E-plane and 56° in the H-plane. Using the approximate formula for the directivity [3] $D \doteq 27\,000/\theta_E\theta_H$ we have $D \doteq 9.9$ dB. A photograph of the device appears in Fig. 1(c).

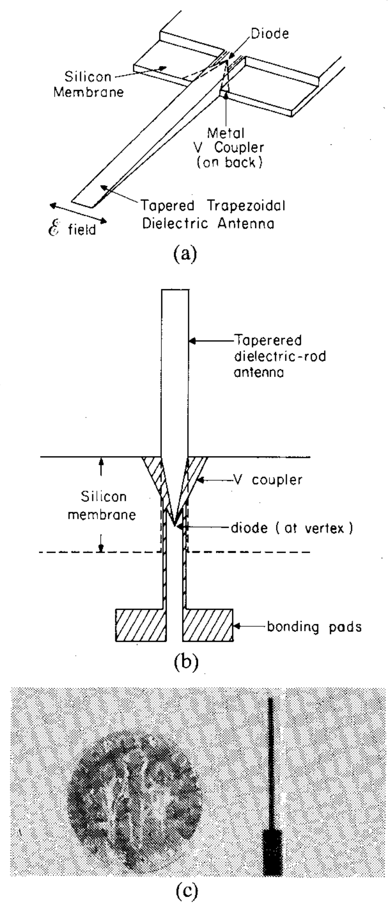

Fig. 1. Monolithic antenna-coupled Schottky mixer. (a) Diagram. (b) Diagram of reverse side showing positions of V-coupler and low-frequency leads. (c) Photograph (U.S. dime for comparison). Diagrams (a) and (b) are not to scale.

The heart of the device is the planar Schottky diode shown in Fig. 2. One arm of the coupler makes ohmic contact to a heavily-doped n^+ region of the substrate. The rectifying contact is made by contacting the other tip of the V-coupler to a neighboring lightly-implanted region. The area of the Schottky contact is made as small as possible (about $3 \cdot 10^{-8}$ cm^2) for low junction capacitance, while the ohmic contact region is shaped to reduce the spreading resistance.

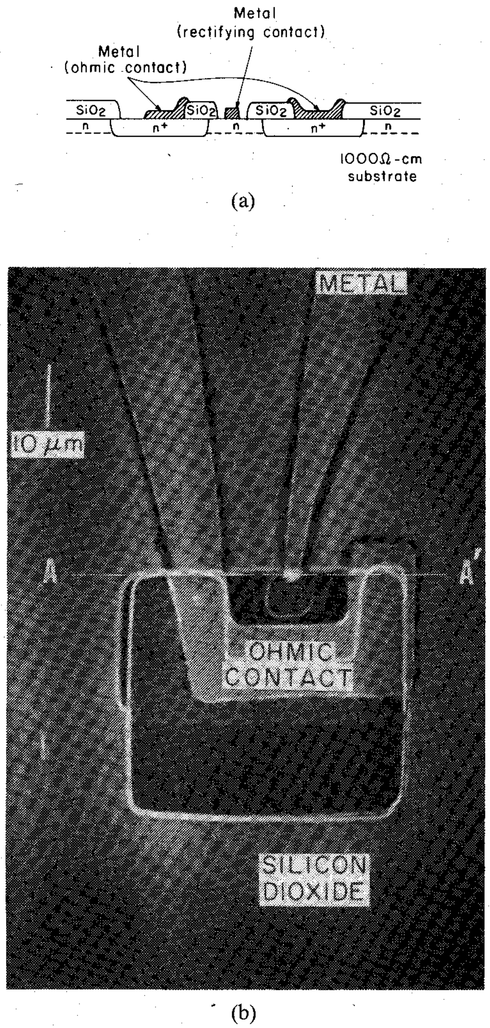

Fig. 2. Surface-oriented Schottky diode. (a) Diagram. (b) Photograph. (a) is a sectional view along the line AA′ shown in Fig. (b).

III. Fabrication

The fabrication process begins with p-type (100) Si wafers with resistivity higher than 1000 $\Omega \cdot$cm. After thermal oxidation of the wafers the waveguide pattern is defined on the back side. This is done by developing a layer of photoresist, then using it as a mask for buffered-HF etching of the SiO_2. The pattern is aligned with the crystal axes in order to obtain smooth planes in the subsequent anisotropic etching procedure. Using the oxide as a mask the wafers are then etched in ethylene-diamine-pyrocatechol-water (EDP) solution until the guides appear. The etching rate is about 50 μm/h at 110°C. A second masking and etching step is then used to produce the thinned region indicated as "silicon membrane" in Fig. 1(a), on the back of which the V coupler will later be deposited.

The diode uses regions of different doping, side by side: a lightly-doped region for the Schottky contact and a heavily-doped region for the ohmic contact as shown in Fig. 2(a). After the wafer is cleaned and thermally oxidized, a window is photolithographically opened on the SiO_2 near the base of the dielectric rod. The opening is then implanted with phosphorus ions at 100 keV and $10^{14}/\text{cm}^2$ dosage, after which there is a two-step annealing [4] which ensures good recrystallization in the implanted region. A subsequent drive-in process produces an n-layer with depth about one micron and concentration $10^{18}/\text{cm}^3$, and simultaneously covers the window with a layer of SiO_2. The heavily-doped region, with doping greater than $10^{20}/\text{cm}^3$, is then defined in a similar way except that, instead of ion implantation, diffusion of impurities is used. It is now necessary to etch a third window in the SiO_2 in order to again expose the lightly-doped and heavily-doped regions for contacting. The wafers are then ready for metallization in a multitarget RF sputtering unit. The system is first evacuated to the 10^{-7}-torr range and sputter-etching is performed in an inert argon atmosphere to remove the interfacial oxide and possible contamination layers. Without breaking the vacuum a uniform Ni film over the entire surface is then sputter-deposited. This metal layer is next removed everywhere except where metallization is needed in the device. An optical projection printing system is used to define the pattern for the V coupler on positive photoresist, which, hardened by baking with a gradual increase in temperature, then serves as a mask for an ion milling procedure. Use of ion milling instead of wet etching reduces undercutting. The hardened photoresist is then removed in an oxygen plasma-asher. About eight identical devices (for this frequency) can be made on a 2-in diameter wafer; the devices are now separated with a scribing machine. The final step is to taper the dielectric waveguides by means of mechanical lapping. Finally, the antennas are polished by light exposure to a $HF:HNO_3:CH_3COOH$ (3:15:5) etch. The finished antennas are about 17 mm long, 0.21 mm high, and 1.1 mm wide at the position of the coupler. The membrane thickness is 0.03 mm.

The diodes made in the above procedure have an estimated zero-bias capacitance of 31 fF. From the static $I-V$ characteristic we find that the series resistance is 350 Ω and the ideality factor is 1.4. The large ideality factor probability results from the high doping used in this nonepitaxial device. The series resistance can of course be greatly reduced if epitaxial material is used.

IV. Performance

The design center frequency of the device was 100 GHz; however, testing was performed at 85 GHz because of availability of a source at that frequency. Since the design is highly insensitive to frequency, performance should be little affected. (At 85 GHz we are near the lowest frequencies at which this kind of device is expected to be useful; earlier work [2] showed that the antenna/waveguide part of the device worked well at frequencies as high as 2500 GHz.) The responsivity of the Schottky diode component can be expected to roll off as ω^{-2} above a cutoff frequency determined by the details of its fabrication. In the present device this cutoff frequency is relatively low, but other workers have demonstrated planar surface-oriented diodes in which the zero-bias cutoff frequency $(2\pi R_s C)^{-1}$ (where

R_s is the dc series resistance and C the zero-bias junction capacitance) is several hundred times higher, in the range 3200–4500 GHz [5].

The 85-GHz klystron radiation source was calibrated by means of a Hughes type 44895H thermistor mount with Hewlett–Packard 432A power meter. (The manufacturer's rated worst-case accuracy for this calibration is 6 percent.) Measurements were then made of video responsivity. Three different methods of in-coupling radiation were tried. In method a), radiation was emitted by a 25-dB standard gain horn and the test device was placed at a distance of 35 cm so that it would receive a nearly plane wave. In this case the power received by the device is expected to be $P = A_e I = \lambda^2 \mathrm{DEI}/4\pi$, where A_e is the antenna's effective area, E its efficiency, and I is the incident intensity [6]. In method b), the tapered dielectric antenna was simply inserted into an untapered section of WR-12 waveguide, so that it became a crude waveguide-dielectric coupler. In method c), an $f/1$ TPX lens, with diameter and nominal focal length each 5 cm, was placed far from the horn to focus the radiation onto the device, which was positioned near the focus for maximum response. Methods a) and b) gave similar maximum responsivities of 33.5 V/W and 35 V/W, respectively. For method c), one would expect signal voltage to increase over method a) by a factor we shall call ρ. Clearly the upper limit of ρ is $\rho_{\max} = TA_L/A_e$, where A_L is the area of the lens and T is its transmission.

In practice ρ will be less than $\rho_{\max}$ because a uniform incident plane wave does not couple ideally to the nonuniform pattern of the dielectric antenna. In our experiment spherical aberration was also present, increasing the size of the lens' focal spot. To study the problem of lens coupling efficiency, additional measurements were performed, using, for convenience, bismuth bolometers [7] in place of Schottky diodes. The transmission of our lens was found to be about 75 percent, giving $\rho_{\max} \doteq 59$. The observed value of ρ was 31. Measurements of the focal spot made by scanning a 2-mm-diameter pyroelectric detector across it gave a good fit of the focal intensity profile to the function e^{-r^2/a^2}, where $a = 3.29$ mm. (This is the value of a after correction for the finite diameter of the pyroelectric detector.) If the lens were ideal, the $1/e$ point of its Airy pattern would occur at $r = 2.61$ mm.

The enlargement of the focal spot is probably due to spherical aberration. We calculate from the observed intensity profile that the ratio of the intensity at the center of the focal spot to the intensity of the unfocused beam is 41. The value of this same ratio, measured by comparing the output of the small pyroelectric detector with and without the lens, is 35. The enlargement of the focal spot due to aberration undoubtedly reduces ρ. Furthermore, the angular beamwidths of the antenna pattern (43° in the E-plane, 38° in the H-plane at the half-power points) are comparable to the angle subtended by the lens (53°), so that some "spillover" occurs. Our conclusion is that the increase of signal using the lens is less than $\rho_{\max}$ primarily because of spherical aberration, and secondarily, because the numerical aperture of the lens is too small. The value of ρ can probably be increased considerably by replacing the lens with an off-axis parabolic reflector.

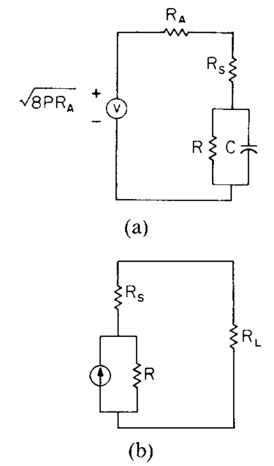

Fig. 3. Circuit models for the Schottky mixer. (a) 85-GHz input circuit. (b) Low-frequency output circuit.

A circuit model for the device is shown in Fig. 3. Fig. 3(a) shows the 85-GHz circuit and Fig. 3(b) the output circuit relevant to dc or the IF frequency. Here R_A is the antenna source impedance (assumed to be real), R_S the diode series resistance, R_L the load resistance and R is the junction incremental resistance, and C the junction capacitance, both measured at the bias point. The voltage responsivity from this model is expected to be

$$\mathfrak{R}_V = \frac{2q}{nkT} \cdot \frac{R_A R^2}{(R + R_S + R_A)^2 + \omega^2 R^2 (R_S + R_A)^2 C^2} \cdot \frac{R_L}{R_L + R_S + R} \quad (1)$$

(where n is the junction's ideality factor). It is difficult to measure R_A; its design value [2] is 100 Ω and we shall assume it has this value. With the values of the junction parameters given in the preceding section and using $C = \sqrt{(q\epsilon N_D)/(2(V_{bi} - V - kT/q))}$ [8] with $V_{bi} = 0.53$ V (the best fit value) we predict voltage responsivity as a function of bias to be as shown in Fig. 4. In this figure the theoretical curves have been multiplied by an efficiency factor E for best agreement with the experimental points obtained using coupling method b). Best fit is obtained with $-10 \log_{10} E = 2.5$ dB. The components of this loss can be estimated. Assuming that dielectric loss arises entirely from the $(1000\ \Omega \cdot \mathrm{cm})^{-1}$ conductivity and occurs, on the average, over half the 1.7-cm length of the antenna, the dielectric loss is approximately $\exp\left[-(1/2)\sigma\sqrt{\mu/\epsilon}\, l\right]$, or 0.35 dB. The electromagnetic coupling loss of the V coupler, according to the microwave simulation of [2], is on the order of 1.0 dB. The difference between the experimentally observed of $-10 \log_{10} E$, which is 2.5 dB, and the sum of the approximate dielectric and coupling loss, which is 1.35 dB, presumably arises from ohmic loss in the metal V coupler; thus ohmic loss amounts to about 1.15 dB. It is

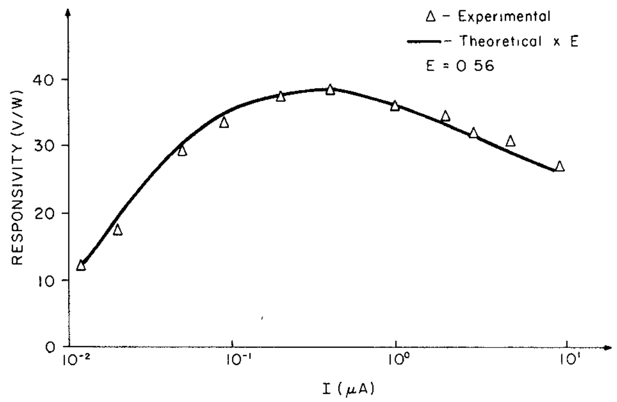

Fig. 4. Voltage responsivity as a function of bias; theoretical curve and experimental points.

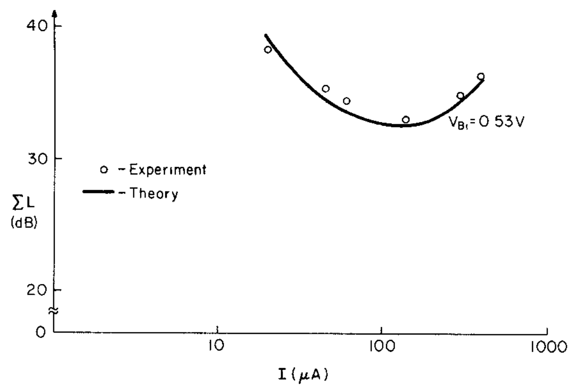

Fig. 5. Total conversion loss as a function of bias; theoretical curve and experimental points.

difficult to estimate how this loss will vary with frequency, owing to the complicated geometry. We note that in our experiment the thickness of the metal film composing the V coupler (100 nm) amounts to only one-fifth of the skin depth.

Measurements were also made of heterodyne conversion efficiency. The output of an 85-GHz local oscillator klystron was combined with the ninth harmonic of another klystron by means of a hybrid coupler and applied to the device using method b). The IF output power at 20 MHz was measured with a calibrated IF amplifier chain. The power of the local oscillator was 10 mW. (Conversion efficiency was near saturation at this power level.) The results are shown in Fig. 5. In order to analyze the performance of the device as a mixer, we need a convenient method for estimating conversion efficiency as a function of the various device parameters. To do this we shall use an ad hoc method that has not been demonstrated rigorously but which does seem to give good agreement with our experiments. We note that the "intrinsic" conversion loss L_0, the conversion loss that would be obtained with perfect input and output matching, no parasitics, and adequate LO power, is typically around 4 dB [9]. To this loss must be added the input mismatch and parasitic loss L_1, and the output mismatch and parasitic loss L_2. The former, which we take to be the ratio of the power dissipated in the junction resistance R to the power available from the antenna is given by

$$L_1 = \frac{4R_A R X_C^2}{R^2(R_A + R_S)^2 + X_C^2(R + R_A + R_S)^2} \tag{2}$$

where $X_C = (j\omega C)^{-1}$. L_2, the ratio of power delivered to the IF amplifier to power available from the mixer at the IF frequency, is given by

$$L_2 = \frac{4RR_L}{(R + R_S + R_L)^2}. \tag{3}$$

The quantity $\Sigma L \equiv -10 \log_{10} (L_0 L_1 L_2 E)$ is plotted against bias in Fig. 5, using a value $E = 2.7$ dB obtained as described above from the responsivity measurements. (The numerical value of E used here is slightly different because a different device was used for these measurements.) Since the value of V_{bi} is not known, a best-fit value of 0.53 V is used. The experimental points agree well with the theoretical curves in order of magnitude, optimum bias, and in the general shapes of the curves. This tends to confirm the approximate technique being used for estimating the conversion efficiency. For bias currents less than the optimum, conversion loss increases because of impedance mismatch; for currents larger than optimum, loss increases primarily because of increasing C.

The very high conversion loss obtained in this preliminary device results largely from the fact that nonepitaxial silicon was used. It is interesting to see what performance could be obtained using approximately the same processing technology, but with epitaxial material consisting of a low-conductivity substrate, high-conductivity buried layer, and a lightly-doped epitaxial layer for the rectifying contact. Taking into account the expected geometrical limitations imposed by fabrication we have estimated the performance of similar structures built in epi-silicon and epi-GaAs. These estimates are shown in Table I. In the "specifications" column, t_1 is the thickness of the buried layer, t_2 the thickness of the epi layer, n_1 the doping of the buried layer, n_2 the doping of the epi, X_C is the estimated capacitive reactance at 100 GHz with forward bias, and A is contact area, in square microns. The IF input resistance R_L is taken to be 50 Ω, and skin effects are neglected. We assume L_0 to be 4 dB. The total overall conversion loss, including coupling losses, is then taken as before to be $L_1 L_2 L_0 E$. We see that the large conversion loss of the present device can be drastically reduced. To allow for additional fabrication difficulty and the need for aligning several devices on the same chip, we choose a contact area of 9 μm (as compared with 3 μm for the present device). The epi-Si version is then predicted to have a more reasonable conversion loss on the order of 15.7 dB. This loss is made up as follows: antenna losses 2.7 dB, input parasitics 5.5 dB, output mismatch 3.5 dB, and "intrinsic" conversion loss 4 dB. For comparison, the loss of a GaAs version is expected to be about 6 dB better, against which must be balanced the possibility of additional technical difficulties to be encountered with this material. The use of epitaxial material requires a new

TABLE I
CONVERSION LOSSES OF PRESENT AND PROPOSED MONOLITHIC MIXERS

Type of diode	Specifications	ohms R_S	ohms X_C	ohms R	dB L_1	dB L_2	dB ΣL
Non-epi silicon (present device)	$A = 3\mu^2$ $n = 10^{18}/cm^3$ $V_{bi} = .53V$ (best fit)	350 (measured)	55	260 (experimental optimum)	17	9	32.7 (theory) 33.5 (exp)
Proposed silicon epi device	$A = 9\mu^2$ $t_1 = 1\mu$ $t_2 = .25\mu$ $n_1 = 10^{20}$ $n_2 = 10^{17}$	60	60	100	5.5	3.5	15.7
Proposed GaAs epi device	$A = 9\mu^2$ $t_1 = 1\mu$ $t_2 = .25\mu$ $n_1 = 5 \cdot 10^{18}$ $n_2 = 10^{17}$	10	60	50	2.3	0.8	9.8

Definitions: L_0 = "intrinsic" conversion loss; L_1 = loss in 85-GHz circuit; L_2 = loss in i.f. circuit; E = efficiency; $\Sigma L = -10 \log_{10} (L_0 L_1 L_2 E)$

fabrication step: the conductive layers must be removed or rendered nonconductive in the waveguide regions, in order to avoid excessive propagation loss. In silicon this would probably be done by etching away the conductive layers. In GaAs one could also use high-energy proton bombardment to reduce the conductivity of the buried layer. To reduce losses from the buried layer to 1 dB/cm its resistivity must be increased to approximately 4800 (t_1/λ) $\Omega \cdot$cm, where λ is the free-space wavelength.

V. CONCLUSIONS

Our results demonstrate the feasibility of near- and submillimeter-integrated circuits combining all-dielectric antennas and waveguides with Schottky diodes. Efficient in-coupling of radiation without the use of conventional metal waveguides has been demonstrated. The various contributions to conversion loss have been estimated, and the conversion loss observed experimentally is in reasonable agreement with these estimations. A similar estimation procedure shows that use of epitaxial silicon can reduce the overall loss of our device (power delivered to IF amplifier ÷ received radiation power) to the order of 16 dB. A similar device made with epi-GaAs would have an overall loss in the neighborhood of 10 dB. Better results could no doubt be obtained with improved technology that could provide better control of epilayer doping and thickness.

The most likely application of integrated devices like these appears to be in short-haul terrestrial communications in the 96-, 140-, and 220-GHz bands. For instance, suppose that due to 16-dB conversion loss the receiver noise temperature is 12 000 K. With a transmitter power of 10 mW at 220 GHz, 10-cm-diameter lenses or mirrors, and a 1-GHz bandwidth, a 10:1 signal-to-noise ratio is obtained over a path of 20 km. Such performance should be acceptable in exchange for the advantage of quantity production at low cost.

REFERENCES

[1] R. M. Knox and P. P. Toulios, "Integrated circuits for the millimeter through optical frequency range," in *Proc. Symp. Submillimeter Waves*, 1970; H. Jacobs and M. M. Chrepta, "Electronic phase shifter for millimeter-wave semiconductor dielectric integrated circuits," *IEEE Trans. Microwave Theory and Tech.*, vol. MTT-22, pp. 411–417, 1974; T. Itoh, "Dielectric waveguide-type millimeter-wave integrated circuits," in *Infrared and Millimeter Waves*, vol. 4, K. Button, Ed. New York: Academic, 1981, ch. 5.

[2] D. B. Rutledge, S. E. Schwarz, T. L. Hwang, D. J. Angelakos, K. K. Mei, and S. Yokota, "Antennas and waveguides for far-infrared integrated circuits," *IEEE J. Quantum Electron.*, vol. QE-16, pp. 508–516, May 1980.

[3] J. Galejs, *Antennas in Inhomogeneous Media*. Oxford: Pergamon Press, 1969.

[4] K. Uda and M. Kamoshida, "Annealing characteristics of highly p$^+$-ion-implanted silicon crystal: Two-Step Anneal," *J. Appl. Phys.*, vol. 48, pp. 18–22, Jan. 1977.

[5] B. J. Clifton, G. D. Alley, R. A. Murphy, and I. H. Mroczkowski, "High-performance quasi-optical GaAs Monolithic mixer at 110 GHz," *IEEE Trans. Electron Devices*, vol. ED-28, pp. 155–157, Feb. 1981.

[6] S. Ramo, J. R. Whinnery, and T. Van Duzer, *Fields and Waves in Communication Electronics*. New York: Wiley, 1965.

[7] T.-L. Hwang, S. E. Schwarz, and D. B. Rutledge, "Microbolometers for infrared detection," *Appl. Phys. Lett.*, vol. 34, pp. 773–776, June 1979.

[8] S. Sze, *Physics of Semiconductor Devices*. New York: Wiley-Interscience 1969.

[9] H. C. Torrey and C. A. Whitmer, *Crystal Rectifiers*. New York: McGraw-Hill, 1948, Fig. 5.13.

Chingchi Yao was born in Taiwan, Republic of China, on November 5, 1950. He received the B.S.E.E. degree from National Taiwan University in 1973, the M.S.E.E. from the University of Pennsylvania in 1976, and the Ph.D. degree in electrical engineering and computer sciences from the University of California, Berkeley, in 1981. He then joined the staff of Advanced Micro Devices, Inc., Sunnyvale, CA, where he is currently involved in development of technology for static RAM's.

Steven E. Schwarz (SM'71) was born in Los Angeles, CA, in 1939. He received the B.S. degree in physics from California Institute of Technology, Pasadena, in 1959, the A.M. from Harvard University, Cambridge, MA, in 1961, and the Ph.D. in electrical engineering from Cal Tech in 1964.

He has held positions with Hughes Research Laboratories, Bell Laboratories, and IBM Research Laboratories. Since 1964 he has been affiliated with the Department of Electrical Engineering and Computer Sciences at the University of California, Berkeley, where he is now a Professor, emphasizing millimeter-wave devices and integrated circuits.

Professor Schwarz held a Guggenheim Fellowship in 1971–72.

B. J. Blumenstock was born in Lisbon, Portugal, on September 12, 1953. He received his undergraduate and graduate training in physics at Michigan State University.

After taking the Ph.D. in 1980, he joined the Electronics Research Laboratory, University of California, Berkeley, as Assistant Research Engineer.

All Solid-State Low-Noise Receivers for 210–240 GHz

JOHN W. ARCHER

Abstract —**Low-noise all solid-state receiver systems for room temperature and cryogenic operation between 210 and 240 GHz are described. The receivers incorporate a single-ended fixed tuned Schottky barrier diode mixer, a frequency-tripled Gunn source as local oscillator and a GaAsFET IF amplifier. Single sideband receiver noise temperatures are typically 1300 K (7.39-dB noise figure) for a room temperature system and 470 K (4.18-dB noise figure) for a cryogenically cooled receiver operating at 20 K.**

I. Introduction

A NUMBER OF researchers have reported the development of heterodyne receiver systems operating at frequencies near 230 GHz [1]–[4]. However, receiver noise figures achieved have been relatively high (typically about 10 dB). Furthermore, the lack of a convenient and reliable local oscillator source with adequate output power has limited the receiver performance, and in many cases necessitated the use of relatively noisy harmonic mixers or complex dual-diode subharmonically pumped devices.

High-performance 210- to 240-GHz receiver systems have recently become practical as a result of significant improvements in single-ended mixer design [5] and the development of efficient frequency multipliers as LO sources [6]. Although receiver noise temperatures can be reduced with mixers and IF amplifiers cooled to 20 K, in many applications it is desirable that the receiver be readily portable and operate at 300 K ambient without the necessary complicated closed cycle helium refrigerators and vacuum systems required for cooled operation. The primary emphasis of this paper concerns the realization of a portable low-noise receiver for room temperature operation between 210–240 GHz. One of the prerequisites for portability was the development of practical solid-state local oscillator sources for this frequency range. Results are also presented which indicate that about a factor of three improvement in receiver noise temperature can be achieved by cooling mixer and IF amplifier to 20 K, but with a necessary increase in complexity and reduced portability.

II. Description of the Receiver and Components

Fig. 1 shows a photograph and block diagram of the ambient temperature receiver. The cooled system is similar except for the inclusion of a small vacuum dewar and closed cycle helium refrigerator[1] in which mixer and IF amplifier are mounted.

A lightweight compact polarizing interferometer diplexer [7] is used for LO/RF combining and filtering. The modular construction of the diplexer (each module forms an 88.9-mm sided aluminum cube) readily enables the implementation of single or dual linearly polarized receivers. The

Manuscript received February 2, 1982; revised March 18, 1982. The National Radio Astronomy Observatory is operated by Associated Universities, Incorporated, under contract with the National Science Foundation.

The author is with the National Radio Astronomy Laboratory, Charlottesville, VA 22903.

[1]CTI Inc., Model 21.

0018-9480/82/0800-1247$00.75 ©1982 IEEE